General flux model in the turbulence driven by multiscale forces

Wei Zhao

State Key Laboratory of Photon-Technology in Western China Energy, International Scientific and Technological Cooperation Base of Photoelectric Technology and Functional Materials and Application, Institute of Photonics and Photon-technology, Northwest University, Xi'an 710127, China

(Received 25 May 2022; accepted 8 August 2022; published 22 August 2022)

In this investigation, the transports of kinetic energy and scalar variance in the turbulence driven by a multiscale force $\boldsymbol{M}\nabla^{\beta}s'$ (which is associated with scalar fluctuations s') are theoretically studied. Although the velocity and scalar fields are strongly coupled, a universal flux conservation equation has been established in wave-number space and exhibits three different solutions, including one real solution and two complex solutions. The numerical analyses show that the turbulence generated under the multiscale force can possess four different cascade processes, including inertial subrange (constant fluxes of kinetic energy and scalar variance), constant-Π_u subrange (quasiconstant flux of kinetic energy), constant-Π_s subrange (quasiconstant flux of scalar variance), and a new subrange with both nonconstant fluxes of kinetic energy and scalar variance in addition to the dissipation subrange. Therefore, much richer information on the cascade processes and scaling exponents can be predicted in such a turbulent system, relative to the well-known Richardson cascade in conventional hydrodynamic turbulence. β is a key to controlling the cascade processes and the scaling exponents. In the constant-Π_u subrange, the slope of velocity spectrum is always $\xi_u = -5/3$, while the slope of the scalar spectrum is $\xi_s = -(6\beta + 1)/3$. In the constant-Π_s subrange, $\xi_u = (4\beta - 11)/5$ and $\xi_s = -(2\beta + 7)/5$. Relying on β, for the real solution, the transport of kinetic energy and scalar variance can be distinguished as four cases. (1) When $\beta < 3/2$ (except $\beta = 2/3$), the constant-Π_u and constant-Π_s subranges could be coexisted, with the former located on the lower wave-number side of the latter. At $\beta = 2/3$, a new inertial subrange with both ξ_u and ξ_s equal to $-5/3$ is present in the multiscale-force dominated subrange. (2) When $3/2 \leqslant \beta < 2$, only the constant-Π_u subrange is predicted. (3) At $\beta = 2$, special and singular exponents of $\xi_u = -1$, $\xi_s = -3$, $\lambda_u = 1$ (the slope of kinetic energy flux), and $\lambda_s = -1$ (the slope of scalar variance flux) can be found, if $MN = 1$. Otherwise, a constant-Π_s subrange is predicted. (4) When $2 < \beta \leqslant 4$, only the constant-Π_s subrange is predicted. For the second solution (one complex solution), when $\beta < 3/2$, there are no constant-Π_u and constant-Π_s subranges, while for $\beta \geqslant 3/2$, a single constant-Π_u subrange is predicted. For the third solution (the other complex solution), there is always a constant-Π_s subrange. Finally, a complete transport picture of both kinetic energy and scalar variance has been established for the type of forced turbulence, which may unify hydrodynamic turbulence, stratified turbulence, turbulent thermal convection and electrokinetic turbulence, etc.

DOI: 10.1103/PhysRevFluids.7.084607

I. INTRODUCTION

Turbulence can be generated by the driving of multiscale forces which are coupled with a scalar field, e.g., in stratified turbulence, magnetohydrodynamic turbulence, electrohydrodynamic turbulence, etc. How the kinetic energy and scalar are transported along with scales in such kind of

scalar-based forced turbulence are still unsolved problems and might remain far from understood for a long while. The kernel is finding the conservative law (or constant quantity) in the transport of kinetic energy and scalar variance in the scalar-based forced turbulence.

A typical example is stratified turbulence. In the 1950s, Bolgiano [1] and Obukhov [2] separately advanced the celebrated BO59 law. The cascade of kinetic energy and temperature variance can both be separated into a series of subranges from large to small scales in sequence, including large-scale injection subrange, buoyancy-driven subrange (in stratified turbulence or turbulent thermal convection [3–5]), inertial subrange and dissipation subrange, etc. In the buoyancy-driven subrange of stably stratified turbulence, the conservative law is that the flux of temperature variance is constant, as inferred by Benzi *et al.* [6]. Thus, the power spectra of velocity and temperature have the following expressions [7,8]:

$$E_u(k) \sim \varepsilon_T^{2/5} f_{\mathrm{VB}}^{4/5} k^{-11/5}, \tag{1a}$$

$$E_T(k) \sim \varepsilon_T^{4/5} f_{\mathrm{VB}}^{-2/5} k^{-7/5}, \tag{1b}$$

where $f_{\mathrm{VB}} = \sqrt{\frac{g}{\langle\rho\rangle}|\frac{d\rho_0}{dz}|}$ is Väisälä-Brunt frequency, where ρ_0, $\langle\rho\rangle$, and g are background density, mean density with perturbations, and gravity respectively. In the inertial subrange, the conservative law becomes that both the fluxes of kinetic energy and temperature variance are constant. Accordingly,

$$E_u(k) \sim \varepsilon_u^{2/3} k^{-5/3}, \tag{2a}$$

$$E_T(k) \sim \varepsilon_u^{-1/3} \varepsilon_T k^{-5/3}. \tag{2b}$$

Similar conservative laws have also been adopted by Zhao and Wang to establish the cascade frameworks of electrokinetic turbulence [9,10] (a branch of turbulence induced electrically, also known as electrohydrodynamic turbulence for a variety of working fluids) and a general form of forced turbulence with $\nabla^{\mathrm{n}} s$-type forces [11], where s is a control scalar for the active turbulent transport process. A series of new scaling phenomena, e.g., $-7/5$ velocity spectrum and $-9/5$ scalar spectrum in electrokinetic turbulence, have been predicted.

However, if we take a look at the investigations above, only three different conservative laws have been reported, relying on the fluxes of kinetic energy and scalar variance. In the inertial subrange, both the fluxes of kinetic energy and scalar variance are constant. In the volume-force-dominated subrange [11], a constant flux of scalar variance with a nonconstant flux of kinetic energy (also known as variable energy flux by Verma [12]) has been reported, while in the dissipation subrange, both the fluxes of kinetic energy and scalar variance are nonconstant. It is curious to ask if there should be a subrange with constant kinetic energy but nonconstant scalar variance. And furthermore, could there be a general conservative law to unify all the conservative laws above?

In 2019, Alam *et al.* [8] revisited the BO59 law by combining the flux of kinetic energy and potential energy (which is essentially related to temperature variance). They suggested considering the summation of kinetic energy flux $[\Pi_u(k)]$ and temperature variance flux $[\Pi_T(k)]$ to be constant, instead of considering each individual to be constant, in the subranges $k \ll k_\eta$ (k_η is the Kolmogorov wave number). A $-5/3$ slope of $E_u(k)$ was found at the lower wave-number side of the buoyancy-driven subrange, where the spectra of temperature variance, i.e., $E_T(k)$, has a slope of $-1/3$. In this subrange, only $\Pi_u(k)$ is approximately constant. Beyond this subrange, the scaling subrange predicted in the BO59 law is found numerically, where only $\Pi_T(k)$ is approximately constant. The investigations of Alam *et al.* [8] (see also Verma [12] who comprehensively reviews the broad applications of variable energy flux) are highly inspiring, as they successfully show the possible existence of constant $\Pi_u(k)$ subrange and the feasibility to complete the jigsaw of cascade in scalar-based forced turbulence.

In this investigation, the model of Zhao and Wang [11] on the forced turbulence with $\nabla^\beta s'$-type forces has been revisited to establish a general conservative law for the forced

turbulence. The research reveals that the inertial subrange and the subranges dominated by $\nabla^\beta s'$-type forces do have a general conservative law or conservation equation. Relying on β, the conservative equation has different solutions, and accordingly, different scaling exponents in the kinetic energy spectrum, scalar spectra, and their corresponding fluxes. Four different cascade processes with either constant or nonconstant fluxes of kinetic energy and scalar variance have been comprehensively predicted. Rich information on characteristic microscales has also been shown.

II. THEORY

In this investigation, a general model of scalar-based forced turbulence [11] with stratified scalar features is investigated by analogy with the analytical method of Alam *et al.* [8]. The turbulent model can be described with the following equations:

$$\frac{Du}{Dt} = -\frac{1}{\rho}\nabla p + \nu\nabla^2\boldsymbol{u} + \boldsymbol{M}\nabla^\beta s', \tag{3a}$$

$$\frac{Ds'}{Dt} = -\boldsymbol{N}\cdot\boldsymbol{u} + D_f\nabla^2 s', \tag{3b}$$

$$\nabla\cdot\boldsymbol{u} = 0, \tag{3c}$$

where ρ is the fluid density, $\boldsymbol{u}$ denotes velocity vector, p is the pressure, and s' is any scalar fluctuations. $\boldsymbol{M}\nabla^\beta s'$ is a multiscale force [12] which is determined by the scalar field s' [11] (more visible in wave-number space as shown later), with $\boldsymbol{M}$ being a certain dimensional vector associated with the physical field and $\nabla^\beta s'$ being a scalar function associated with a specific βth-order derivative of the scalar s'. $\boldsymbol{N}$ is a vector related to scalar s to characterize the feature of stratified scalar background, and ν and D_f are the kinematic viscosity and diffusivity of the scalar respectively. Equations (3a) and (3b) require that $\boldsymbol{M}$ and $\boldsymbol{N}$ have the dimensions of $U^2\,L^{\beta-1}\,S^{-1}$ and S/L, where U, L, and S represent the dimensions of velocity, length, and scalar respectively. For buoyancy-driven turbulence, with $s' = \rho' g f_{\mathrm{VB}}^{-1}\langle\rho\rangle^{-1}$ being density fluctuations, $\beta = 0$, $\boldsymbol{M} = \boldsymbol{N} = -f_{\mathrm{VB}}\hat{\boldsymbol{z}}$, Eqs. (3a) and (3b) are consistent with Alam *et al.* [8]. For electrokinetic turbulence with a quasistratified mean scalar field, it can be $\beta = 1$, $\boldsymbol{M} = -\varepsilon E^2\hat{\boldsymbol{y}}/\rho\langle\sigma\rangle$, $\boldsymbol{N} = \nabla\langle\sigma\rangle$, where σ is the electric conductivity and E is the electric field in the y direction ($\hat{\boldsymbol{y}}$) perpendicular to the initial interface of electric conductivity [13,14].

Here, the turbulent flow is hypothesized to be homogeneous and isotropic, e.g., by the modulation of pressure [15], to simplify the theoretical analysis. Therefore, according to Verma [12,16,17], the governing equations in Fourier space can be

$$\frac{d}{dt}E_u(\boldsymbol{k}) = T_u(\boldsymbol{k}) + F_s(\boldsymbol{k}) - D_u(\boldsymbol{k}), \tag{4a}$$

$$\frac{d}{dt}E_s(\boldsymbol{k}) = T_s(\boldsymbol{k}) - F_A(\boldsymbol{k}) - D_s(\boldsymbol{k}), \tag{4b}$$

where $\boldsymbol{k}$ is the wave vector and $E_u(\boldsymbol{k}) = \frac{1}{2}|\boldsymbol{u}(\boldsymbol{k})|^2$ and $E_s(\boldsymbol{k}) = \frac{1}{2}|s'(\boldsymbol{k})|^2$ are the modal kinetic energy and scalar variance. $T_u(\boldsymbol{k})$ and $D_u(\boldsymbol{k})$ are the nonlinear kinetic energy transfer rate and dissipation rate, respectively. $T_s(\boldsymbol{k})$ and $D_s(\boldsymbol{k})$ are the nonlinear transfer rate of scalar variance and scalar dissipation rate, respectively. $F_s(\boldsymbol{k})$ denotes the energy feeding rate by the multiscale force and $F_A(\boldsymbol{k})$ is the scalar feeding rate by bulk components. These quantities can be expressed as

$$T_u(\boldsymbol{k}) = \sum_m \mathrm{Im}\{[\boldsymbol{k}\cdot\boldsymbol{u}(\boldsymbol{n})][\boldsymbol{u}(\boldsymbol{m})\cdot\boldsymbol{u}^*(\boldsymbol{k})]\}, \tag{5a}$$

$$T_s(\boldsymbol{k}) = \sum_m \mathrm{Im}\{[\boldsymbol{k}\cdot\boldsymbol{u}(\boldsymbol{n})][s'(\boldsymbol{m})s'^*(\boldsymbol{k})]\}, \tag{5b}$$

$$F_s(\boldsymbol{k}) = \mathrm{Re}[(\boldsymbol{M}\nabla^\beta s')(\boldsymbol{k}) \cdot \boldsymbol{u}^*(\boldsymbol{k})] = \mathrm{Re}[s'(\boldsymbol{k})k^\beta \boldsymbol{M} \cdot \boldsymbol{u}^*(\boldsymbol{k})], \tag{5c}$$

$$F_A(\boldsymbol{k}) = \mathrm{Re}[s'(\boldsymbol{k})\boldsymbol{N} \cdot \boldsymbol{u}^*(\boldsymbol{k})], \tag{5d}$$

$$D_u(\boldsymbol{k}) = 2\nu k^2 E_u(\boldsymbol{k}), \tag{5e}$$

$$D_s(\boldsymbol{k}) = 2D_f k^2 E_s(\boldsymbol{k}), \tag{5f}$$

where Re and Im represent the real and imaginary parts of the quantity. $\boldsymbol{k} = \boldsymbol{m} + \boldsymbol{n}$. Equation (5c) is not a strict mathematically derivation, but a dimensional one. Its explicit form should be derived based on the definition of the operator ∇^β, even though the major purpose of applying the $\boldsymbol{M}\nabla^\beta s'$ type force in this investigation can be seen in Eq. (5c). Generally, people can assume $F_s(\boldsymbol{k})$ to have a form of $\mathrm{Re}[s'(\boldsymbol{k})\boldsymbol{W}(k) \cdot \boldsymbol{u}^*(\boldsymbol{k})]$, which is established on the basis of the cospectra $s'(\boldsymbol{k})\boldsymbol{u}^*(\boldsymbol{k})$ and a coupling function $\boldsymbol{W}(k)$ which can be expanded polynomially as $\boldsymbol{W}(k) = \sum_{n=0}^{\infty} \boldsymbol{a_n} k^n$ (where n is an integer). Then, the contribution of the dominant nth-order term can be estimated through $\mathrm{Re}[s'(\boldsymbol{k})\boldsymbol{a_n}k^n \cdot \boldsymbol{u}^*(\boldsymbol{k})]$. However, if there exist some neighboring orders (e.g., $\boldsymbol{a}_0 + \boldsymbol{a}_1 k$) that all exhibit important contributions to the energy feeding rate, one may use a simple power-law equation $\boldsymbol{a_\beta} k^\beta$ with a noninteger exponent to approximate the polynomial terms. Therefore, by taking into account both integer and noninteger orders above, and distinguishing the influence of the dominant order on the transport of kinetic energy and scalar variance, the $\boldsymbol{M}\nabla^\beta s'$ force is adopted in this investigation.

In a spherical shell around $k = |\boldsymbol{k}|$ with a thickness of dk in the wave-number space, Eqs. (4a) and (4b) become

$$\sum_{k<|\boldsymbol{k}'|\leqslant k+dk} \frac{d}{dt} E_u(\boldsymbol{k}') = \sum_{k<|\boldsymbol{k}'|\leqslant k+dk} [T_u(\boldsymbol{k}') + F_s(\boldsymbol{k}') - D_u(\boldsymbol{k}')], \tag{6a}$$

$$\sum_{k<|\boldsymbol{k}'|\leqslant k+dk} \frac{d}{dt} E_s(\boldsymbol{k}') = \sum_{k<|\boldsymbol{k}'|\leqslant k+dk} [T_s(\boldsymbol{k}') - F_A(\boldsymbol{k}') - D_s(\boldsymbol{k}')]. \tag{6b}$$

According to Alam *et al.* [8] and Verma [12], the flux of kinetic energy $\Pi_u(k) = -\sum_{|\boldsymbol{k}'|\leqslant k} T_u(\boldsymbol{k}')$ and the flux of scalar variance $\Pi_s(k) = -\sum_{|\boldsymbol{k}'|\leqslant k} T_s(\boldsymbol{k}')$. It simply yields

$$d\Pi_u(k) = -\sum_{k\leqslant|\boldsymbol{k}'|\leqslant k+dk} T_u(\boldsymbol{k}'), \tag{7a}$$

$$d\Pi_s(k) = -\sum_{k\leqslant|\boldsymbol{k}'|\leqslant k+dk} T_s(\boldsymbol{k}'), \tag{7b}$$

Furthermore,

$$E_u(k)dk = \sum_{k<|\boldsymbol{k}'|\leqslant k+dk} E_u(\boldsymbol{k}'), \tag{8a}$$

$$E_s(k)dk = \sum_{k<|\boldsymbol{k}'|\leqslant k+dk} E_s(\boldsymbol{k}'), \tag{8b}$$

$$F_s(k)dk = \sum_{k<|\boldsymbol{k}'|\leqslant k+dk} F_s(\boldsymbol{k}'), \tag{8c}$$

$$F_A(k)dk = \sum_{k<|\boldsymbol{k}'|\leqslant k+dk} F_A(\boldsymbol{k}'), \tag{8d}$$

$$D_u(k)dk = \sum_{k<|\boldsymbol{k}'|\leqslant k+dk} D_u(\boldsymbol{k}'), \tag{8e}$$

$$D_s(k)dk = \sum_{k<|\boldsymbol{k}'|\leqslant k+dk} D_s(\boldsymbol{k}'), \tag{8f}$$

where $E_u(k)$ is the power spectrum of kinetic energy, $E_s(k)$ is the power spectrum of scalar variance, $F_s(k)$ is the energy feeding rate by multiscale force at wave number k, $F_A(k)$ is the scalar feeding rate at wave number k, and D_u and D_s are dissipation terms at wave number k respectively. After substituting Eqs. (7a) and (7b) and (5a)–(5f) to Eqs. (6a) and (6b), considering the flow is statistically equilibrium, and letting $dk \to 0$, it is obtained that

$$\frac{d}{dk}\Pi_u(k) = F_s(k) - D_u(k), \tag{9a}$$

$$\frac{d}{dk}\Pi_s(k) = -F_A(k) - D_s(k), \tag{9b}$$

where $F_s(k) = \mathrm{Re}[s'(k)k^\beta \boldsymbol{M}\cdot\boldsymbol{u}^*(k)]$, $F_A(k) = \mathrm{Re}[s'(k)\boldsymbol{N}\cdot\boldsymbol{u}^*(k)]$, $D_u(k) = 2\nu k^2 E_u(k)$, and $D_s(k) = 2D_f k^2 E_s(k)$. Thus, if $\boldsymbol{M}$ is parallel to $\boldsymbol{N}$,

$$F_s(k) - \frac{M}{N}F_A(k)k^\beta = 0, \tag{10}$$

where $M = |\boldsymbol{M}|$ and $N = |\boldsymbol{N}|$ respectively.

In the inertial subrange, where the influence of multiscale forcing and dissipation is negligible, Eqs. (9a) and (9b) become

$$\frac{d}{dk}\Pi_u(k) = 0, \tag{11a}$$

$$\frac{d}{dk}\Pi_s(k) = 0, \tag{11b}$$

or

$$\Pi_u(k) = \text{const along } k, \tag{12a}$$

$$\Pi_s(k) = \text{const along } k. \tag{12b}$$

The inertial subrange must have constant Π_u and Π_s.

In the subrange where the transports of kinetic energy and scalar variance are dominated by the multiscale force, say the multiscale-force dominated (MFD) subrange, the dissipation terms of kinetic energy and scalar variance are ignored. Equations (9a) and (9b) become

$$\frac{d}{dk}\Pi_u(k) = F_s(k), \tag{13a}$$

$$\frac{d}{dk}\Pi_s(k) = -F_A(k). \tag{13b}$$

Combining Eqs. (10), (13a), and (13b), a conservation law is thus obtained:

$$\frac{d}{dk}\Pi_u(k) + \frac{M}{N}k^\beta\frac{d}{dk}\Pi_s(k) = 0. \tag{14}$$

It can be seen that Eqs. (12a) and (12b) that represent constant fluxes of kinetic energy and scalar variance are the special solutions of Eq. (14). The scenarios of Kolmogorov [18,19] and Obukhov

and Corrsin [20,21] theories have been unified into the model. According to Alam *et al.* [8],

$$E_u(k) = u_k^2/k, \tag{15a}$$

$$E_s(k) = s_k^2/k, \tag{15b}$$

$$\Pi_u(k) = k u_k^3, \tag{15c}$$

$$\Pi_s(k) = k s_k^2 u_k. \tag{15d}$$

Substituting $\Pi_u(k)$ and $\Pi_s(k)$ into Eq. (14) above,

$$\frac{d}{dk} k u_k^3 + \frac{M}{N} k^\beta \frac{d}{dk} k s_k^2 u_k = 0. \tag{16}$$

When $\beta = 0$ and $M = N = -f_{\mathrm{VB}}$, Eq. (16) is equivalent to Eq. (17) in the paper of Alam *et al.* [8] for stratified turbulence. Considering in the MFD subrange, the flow is driven by the $\boldsymbol{M}\nabla^\beta s'$ type force, dimensionally $k u_k^2 = k^\beta M s_k$, then Eq. (16) becomes

$$u_k + \frac{(3-2\beta)}{MN} k^{2-\beta} u_k^3 + \left(3k + \frac{5}{MN} k^{3-\beta} u_k^2\right) \frac{du_k}{dk} = 0. \tag{17}$$

Equation (17) is a universal equation for the MFD subrange in the forced turbulence driven by $\boldsymbol{M}\nabla^\beta s'$ type force. There are three solutions in Eq. (17), including one real solution and two complex solutions. Here, all three solutions are taken into account, say $u_{k,i}^2 = u_{k,i} u_{k,i}^*$ with $u_{k,i}^*$ being the complex conjugate of $u_{k,i}$ which is the ith solution of Eq. (17). Thus, Eqs. (15a)–(15d) can be simply rewritten as

$$E_u(k) = k^{-1}(u_k u_k^*) \sim k^{\xi_u}, \tag{18a}$$

$$E_s(k) = M^{-2} k^{3-2\beta} E_u^2(k) \sim k^{\xi_s}, \tag{18b}$$

$$\Pi_u(k) = k^{5/2} E_u^{3/2}(k) \sim k^{\lambda_u}, \tag{18c}$$

$$\Pi_s(k) = M^{-2} k^{\frac{11}{2}-2\beta} E_u^{5/2}(k) \sim k^{\lambda_s}, \tag{18d}$$

where ξ_u, ξ_s, λ_u, λ_s denote the scaling exponents of E_u, E_s, Π_u, and Π_s respectively.

III. NUMERICAL RESULTS

Equation (17) can be solved numerically after settling β, M, and N. Nevertheless, to directly simulate Eq. (17) in a wide wave-number range, e.g., from 10^{-5} to 10^{25}, the cost of computation is unaffordable in linear wave-number space. Therefore, it is necessary to make a transform from the linear wave-number space to the log space (or decades), i.e., $k = 10^q$; thus Eq. (17) becomes

$$u_k + \frac{(3-2\beta)}{MN} 10^{q(2-\beta)} u_k^3 + \frac{1}{\ln 10}\left[3 + \frac{5}{MN} 10^{q(2-\beta)} u_k^2\right] \frac{du_k}{dq} = 0. \tag{19}$$

In the q space, this equation can be solved simply with

$$u_{k,\,i,\,m} + \frac{(3-2\beta)}{MN} 10^{q_m(2-\beta)} u_{k,\,i,\,m}^3 + \frac{1}{\ln 10}\left[3 + \frac{5}{MN} 10^{q_m(2-\beta)} u_{k,\,i,\,m}^2\right] \frac{u_{k,\,i,\,m} - u_{k,i,m-1}}{q_m - q_{m-1}} = 0 \tag{20}$$

for $m = 2,\ 3,\ \ldots,\ m_{\max}$, where $m_{\max}$ is the maximum index of the decade q_m in this investigation. $u_{k,\,i,m}(q_m)$ denotes the $u_{k,i}$ at q_m, or the equivalent wave number $k_m = 10^{q_m}$. Apparently, the solution of Eq. (19) relies on an initial $u_{k,i}$ at $m = 1$, i.e., $u_{k,i,1}$. Considering that the total kinetic energy $\int E_u(k)dk$ is inevitably determined by MN, the distribution of u_k (including $u_{k,i,1}$) relies on MN as well. The influence of β, MN, and the initial value $u_{k,1,1}$ of the first (real) solution will be comprehensively discussed in the following sections.

A. Influence of β

According to Eq. (17), it is explicitly seen that β is a crucial parameter in determining the transport of kinetic energy and scalar variance. Zhao and Wang [11] theoretically predicted that β should be no more than 4, otherwise, the statistical equilibrium of the system can be broken, as a result of unlimited accumulation of kinetic energy at small scales. Although the conclusion is attributed to a constant flux of scalar variance which is absent in some cases, the restriction (i.e., $\beta \leqslant 4$) is still applicable as discussed in Sec. IIIB.

1. $\beta < 3/2$

Generally, when $\beta < 3/2$ (except $\beta = 2/3$), the MFD subrange can always be separated into two additional subranges (Fig. 1). One has a quasiconstant flux of kinetic energy (say "constant-Π_u" subrange), and the other has a quasiconstant flux of scalar variance (say "constant-Π_s" subrange). The two subranges intersect with each other at a critical wave number k_{ci}.

(i) Constant-Π_u subrange. Figure 1(a) shows the variation of $E_u(k)$ versus β in a large wave-number range. When $\beta < 3/2$ (except $\beta = 2/3$), $\xi_u = -5/3$ and $\lambda_u \sim 0$ [Fig. 1(c)] can be found in the lower wave-number range of $k \ll k_{ci}$. Since λ_u is not exactly zero, but has a very small ($\sim$1/30 or smaller) magnitude which is negligible, it is called "quasiconstant." This explains why Π_s can be nonconstant [Fig. 1(d)] according to Eq. (14).

In the constant-Π_u subrange, $E_s(k)$ shows a new scaling behavior which relies on β, as plotted in Fig. 1(b). ξ_s is linearly related to β as

$$\xi_s = -(6\beta + 1)/3. \tag{21}$$

The flux of scalar variance has a scaling exponent as

$$\lambda_s = (4 - 6\beta)/3. \tag{22}$$

Since $\lambda_u = 0$ and $\lambda_s = (4-6\beta)/3$, according to Eqs. (13), it is obtained that $F_s(k) \sim k^{-1}$ and $F_A(k) \sim k^{(1-6\beta)/3}$.

(ii) Constant-Π_s subrange. When $\beta < 3/2$(except $\beta = 2/3$), as shown in Fig. 1(d), the constant-Π_s subrange where $\lambda_s \sim 0$ is found located at the higher wave-number range of the constant-Π_u subrange, i.e., $k \gg k_{ci}$. From the numerical calculation, it is found that ξ_u in the constant-Π_s subrange follows

$$\xi_u = (4\beta - 11)/5. \tag{23}$$

This is explicitly consistent with the theory of Zhao and Wang [11], which assumes that $\Pi_s(k)$ is constant. The corresponding scaling exponents of $\Pi_u(k)$ become

$$\lambda_u = (6\beta - 4)/5, \tag{24}$$

which can be either positive or negative. Equation (24) indicates that the constant-Π_s subrange has clearly variable energy flux [12]. Since λ_s is approximately zero (below 1/40), $\Pi_s(k)$ is quasiconstant in the constant-Π_s subrange. Here, ξ_s is linearly related to β as

$$\xi_s = -(2\beta + 7)/5, \tag{25}$$

which is also consistent with the predictions by Zhao and Wang [11]. In the constant-Π_s subrange, since $\lambda_u = (6\beta-4)/5$ and $\lambda_s = 0$, according to Eqs. (13), it is obtained that $F_s(k) \sim k^{(6\beta-9)/5}$ and $F_A(k) \sim k^{-1}$.

(iii) Special case at $\beta = 2/3$. From Fig. 1, it is interesting to see a special case at $\beta = 2/3$, under which $\xi_u = \xi_s = -5/3$ and $\lambda_u = \lambda_s = 0$ in the MFD subrange. This means that, at this β, there exists a delicate balance among the multiscale force, the transport of kinetic energy, and scalar variance, which makes both kinetic energy and scalar variance experience inertial cascades from large to small scales. This result can be predicted if rewriting Eq. (14) as $\frac{d}{dk}\Pi_u(k) +$

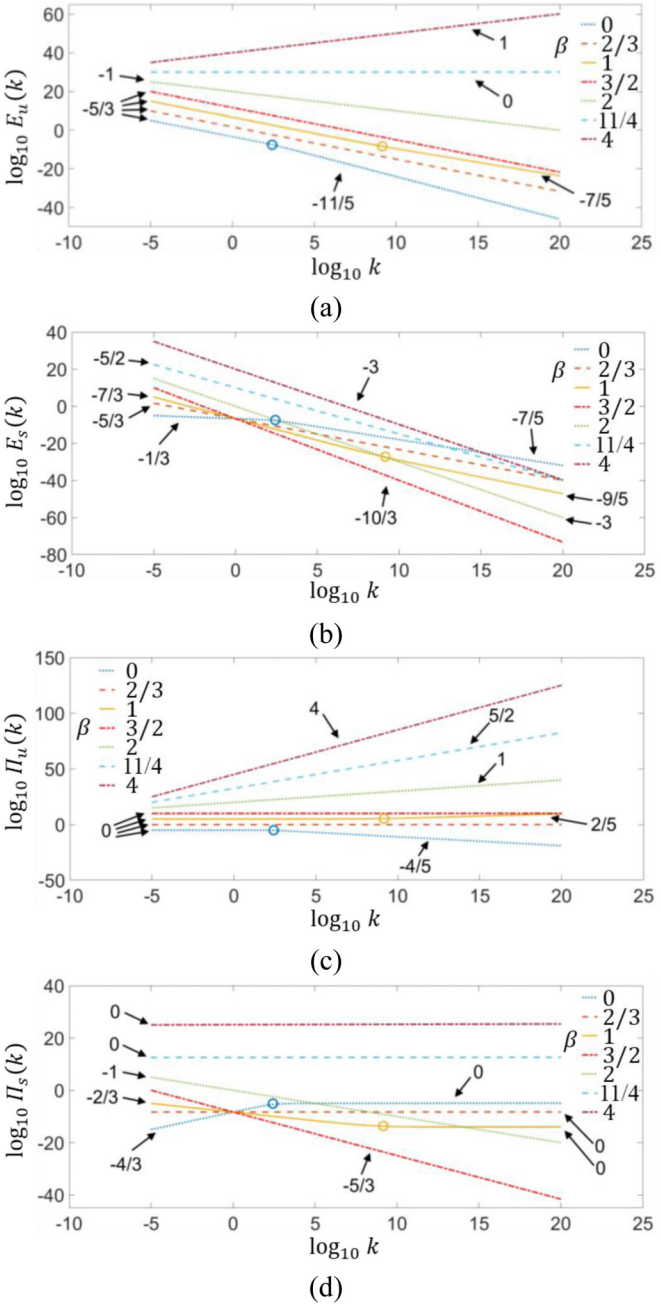

FIG. 1. Influence of β on the transport of kinetic energy and scalar variance, where $MN = 1$ and only the first solution (real solution), i.e., $u_{k,1}$, has been taken into account. The initial value $u_{k,1,1} = 1$. (a) Power spectra of kinetic energy E_u. Each curve has been shifted by 5 vertically for better clarity. (b) Power spectra of scalar variance E_s. (c) Flux of kinetic energy Π_u. Each curve has been shifted by 5 vertically for better clarity. (d) Flux of scalar variance Π_s.

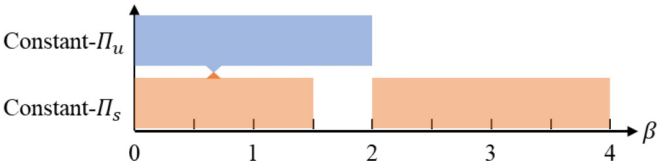

FIG. 2. Relationship between β and the energy or scalar transport subranges. The blue bar shows the constant-Π_u subrange and the orange one shows the constant-Π_s subrange. The small triangles highlight $\beta = 2/3$, where the constant-Π_u and constant-Π_s subranges overlap. For the real solution only.

$\frac{1}{MN}k^{\beta}\frac{d}{dk}[k^{(4/3)-2\beta}\Pi_u(k)^{(5/3)}] = 0$, since $\Pi_s(k) = M^{-2}k^{(4/3)-2\beta}\Pi_u(k)^{(5/3)}$. To make the equation established, both $\Pi_u(k) = \text{const}$ and $k^{(4/3)-2\beta} = \text{const}$ are required. Accordingly, $\beta = 2/3$. The result indicates that, on one hand, the direct observations of constant fluxes of kinetic energy and scalar variance, and the corresponding $-5/3$ slopes in the spectra of kinetic energy and scalar variance, are insufficient to ensure the existence of the Kolmogorov law [18,19] and the Obukhov-Corrsin law [20,21] in scalar-based forced turbulence. On the other hand, it is possible to significantly extend the width of the inertial subrange by generating forced turbulence with $\beta = 2/3$.

2. $3/2 \leqslant \beta < 2$

In the investigations of Zhao and Wang [11], they found that $\beta = 3/2$ is a special value on which the second-order structure function of velocity becomes irrelevant to scales, if constant-Π_s is hypothesized. However, their prediction shows a departure in the range of $3/2 \leqslant \beta < 2$. From Fig. 1, it can be seen that $\beta = 3/2$ is a critical value beyond which the coexistence of constant-Π_u and constant-Π_s subranges is broken. In the MFD subrange, only the constant-Π_u subrange is observed, where $\xi_u = -5/3$ and $\lambda_u = 0$. ξ_s and λ_s can be calculated from Eqs. (21) and (22).

3. $\beta = 2$

$\beta = 2$ is a special and singular case in this investigation. In this case, no constant-Π_u or constant-Π_s subrange was observed. The scaling exponents are $\xi_u = -1$, $\xi_s = -3$, $\lambda_u = 1$, and $\lambda_s = -1$ respectively. All the derivatives of the scaling exponents, e.g., $d\xi_u/d\beta$ and $d\xi_s/d\beta$, are not available, since ξ_u, ξ_s, λ_u, and λ_s are all discontinuous at $\beta = 2$. However, as illustrated in Sec. IV, $\beta = 2$ is a special case only at $MN = 1$. In any practical application, since MN cannot be exactly unity, the special case may not be observed.

4. $2 < \beta \leqslant 4$

When β is further increased, the constant-Π_s subrange returns with $\lambda_s = 0$, as can be seen from Fig. 1(d). In contrast, the constant-Π_u subrange disappears in the entire wave-number range investigated. In this β range, ξ_u, λ_u, and ξ_s can be again calculated on the basis of Eqs. (23)–(25).

Generally, as shown in Fig. 2, when $\beta < 3/2$ or $2 < \beta \leqslant 4$, the constant-Π_s subrange is observed in the wavenumber range, where the theoretical predictions of Zhao and Wang [11] can be applied. When $0 \leqslant \beta < 2$ or $\beta = 2$ with $MN \neq 1$, the constant-Π_u subrange is predictable. The detailed relations between the scaling exponents and β have also been summarized in Table I.

B. Influence of the magnitude of MN and $u_{k,1,1}$

MN is a quantity to evaluate the forced convection effect in the scalar-based forced turbulence. According to Eq. (17), M and N have no difference in the scaling behavior of u_k and the related quantities. However, M does affect the magnitudes of $E_s(k)$ and Π_s from Eqs. (18b) and (18d). For better comparison, the magnitude of MN is changed through M, and $N = 1$ is unchanged.

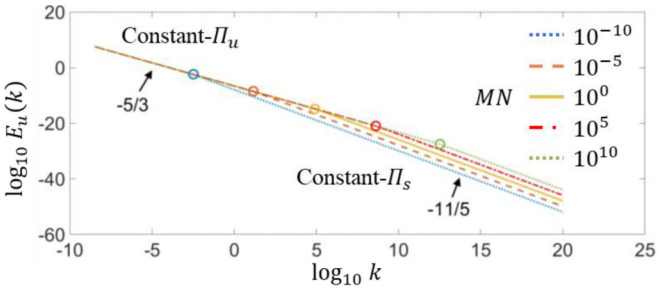

(a)

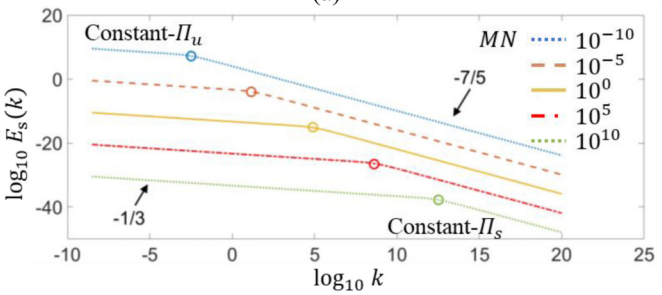

(b)

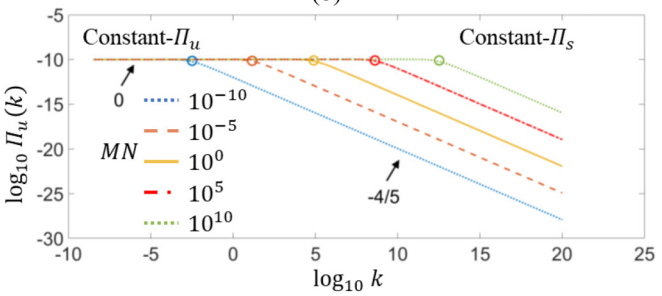

(c)

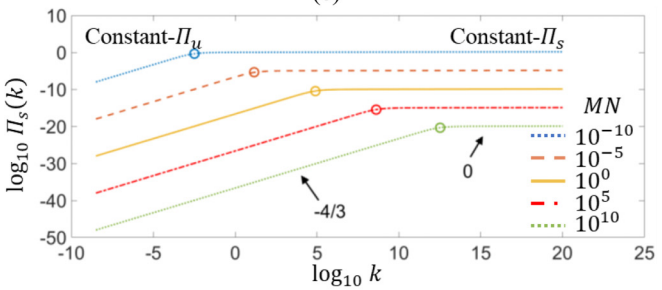

(d)

FIG. 3. Influence of MN on the transport of kinetic energy and scalar variance, where $\beta = 0$. Here, only the first solution (real solution), i.e., $u_{k,1}$, has been taken into account. The initial value $u_{k,1,1} = 1$. The colored circles denote the position of k_{ci}. (a) Power spectra of kinetic energy E_u. (b) Power spectra of scalar variance E_s. (c) Flux of kinetic energy Π_u. (d) Flux of scalar variance Π_s.

TABLE I. Transport of kinetic energy and scalar variance in the MFD subrange of the scalar-based forced turbulence.

MFD subranges		Π_u	Π_s	E_u	E_s	Range of β
1st solution	constant-Π_u	$\sim k^0$	$k^{(4-6\beta)/3}$	$k^{-5/3}$	$k^{-(6\beta+1)/3}$	$\begin{cases} 0 \leqslant \beta < 2 \\ \beta = 2 \text{ and } MN \neq 1 \end{cases}$
	constant-Π_s	$k^{(6\beta-4)/5}$	$\sim k^0$	$k^{(4\beta-11)/5}$	$k^{-(2\beta+7)/5}$	$\begin{cases} \beta < 3/2 \\ 2 < \beta \leqslant 4 \end{cases}$
	special case 1	k^0	k^0	$k^{-5/3}$	$k^{-5/3}$	$\beta = 2/3$
	special case 2	k	k^{-1}	k^{-1}	k^{-3}	$\beta = 2$ and $MN = 1$
2nd solution	special case 3	$k^{(3\beta-4)/2}$	$k^{(\beta-4)/2}$	$k^{\beta-3}$	k^{-3}	$\beta < 3/2$
	constant-Π_u	$\sim k^0$	$k^{(4-6\beta)/3}$	$k^{-5/3}$	$k^{-(6\beta+1)/3}$	$\beta \geqslant 3/2$
3rd solution	constant-Π_s	$k^{(6\beta-4)/5}$	$\sim k^0$	$k^{(4\beta-11)/5}$	$k^{-(2\beta+7)/5}$	$\beta < 4$

(i) When $\beta = 0$, from Fig. 3(a), it can be seen in the constant-Π_u subrange that $\xi_u = -5/3$, $\xi_s = -1/3$, $\lambda_u = 0$, and $\lambda_s = 4/3$, while in the constant-Π_s subrange, $\xi_u = -11/5$, $\xi_s = -7/5$, $\lambda_u = -4/5$, and $\lambda_s = 0$. All these data are consistent with the numerical investigations of Alam *et al.* [8] on stably stratified turbulence and again support the effectiveness of the current model.

As MN is increased, the critical wave number k_{ci} increases rapidly (see Fig. 3), which indicates that the constant-Π_u subrange invades the constant-Π_s subrange and pushes it towards the higher wave-number region. There is also no crossover observed between the MFD subrange and the inertial subrange in the investigated wave-number region. Alam *et al.* [8] attributed the absence of inertial subrange to the insufficient strong disturbing from buoyancy. However, from Eq. (17), it can be predicted that if Π_u and Π_s are constants, there is only one nontrivial solution of u_k that can be observed at $\beta = 2/3$. Equation (17) that established for the MFD subrange is not applicable for the inertial subrange. This is because during the derivation of Eq. (17) from Eq. (16), an additional condition $ku_k^2 = k^\beta Ms_k$ which only applies in the MFD subrange has been applied. Thus, it is reasonable that people cannot observe an intersection between the MFD and inertial subrange on the basis of Eq. (17). A similar conclusion should also apply to the investigation of Alam *et al.* [8].

Increasing MN also leads to a decrease of E_s and Π_s. This result is unreasonable and can be attributed to the fixed $u_{k,1,1}$ in the numerical calculation.

(ii) When MN is changed, $u_{k,1,1}$, which is related to E_u, E_s, Π_u, and Π_s curves at a large scale, should also be changed accordingly. Or in other words, $u_{k,1,1}$ is a function of MN. Figure 4 shows the influence of $u_{k,1,1}$ on the E_u, E_s, Π_u, and Π_s curves at $\beta = 0$. As $u_{k,1,1}$ is increased, the critical wave number k_{ci} decreases rapidly, which indicates that the constant-Π_s subrange invades the constant-Π_u subrange and pushes it towards the lower wave-number region. In the meanwhile, the magnitudes of E_u, E_s, Π_u, and Π_s all increase with $u_{k,1,1}$.

(iii) The influence of β on the relation between MN and k_{ci} has been plotted in Fig. 5(a). In the log-log plot, all the curves exhibit a linear relationship, which indicates $k_{ci} \sim (MN)^\varphi$, where $\varphi = \varphi(\beta)$ is the scaling exponent relying on β. As β is increased from 0 to 1, φ increases rapidly from 0.75 (at $\beta = 0$) to 2.91 (at $\beta = 1$), as shown in Fig. 5(c). The increase of φ alongside β is highly nonlinear and follows a quasiexponential way. When $\beta = 5/4$, φ is increased to an extraordinarily high value at 11.3. In other words, if MN is doubled, k_{ci} is increased 2400 times.

Figure 5(b) shows the influence of $u_{k,1,1}$ on k_{ci}. It is found that k_{ci} changes with $u_{k,1,1}$ as $k_{ci} \sim u_{k,1,1}^\psi$, with $\psi = \psi(\beta)$ being another exponent relying on β. Relative to φ which are always positive, ψ are all negative with exactly the twice the magnitude of φ, as compared in Fig. 5(c). As β is

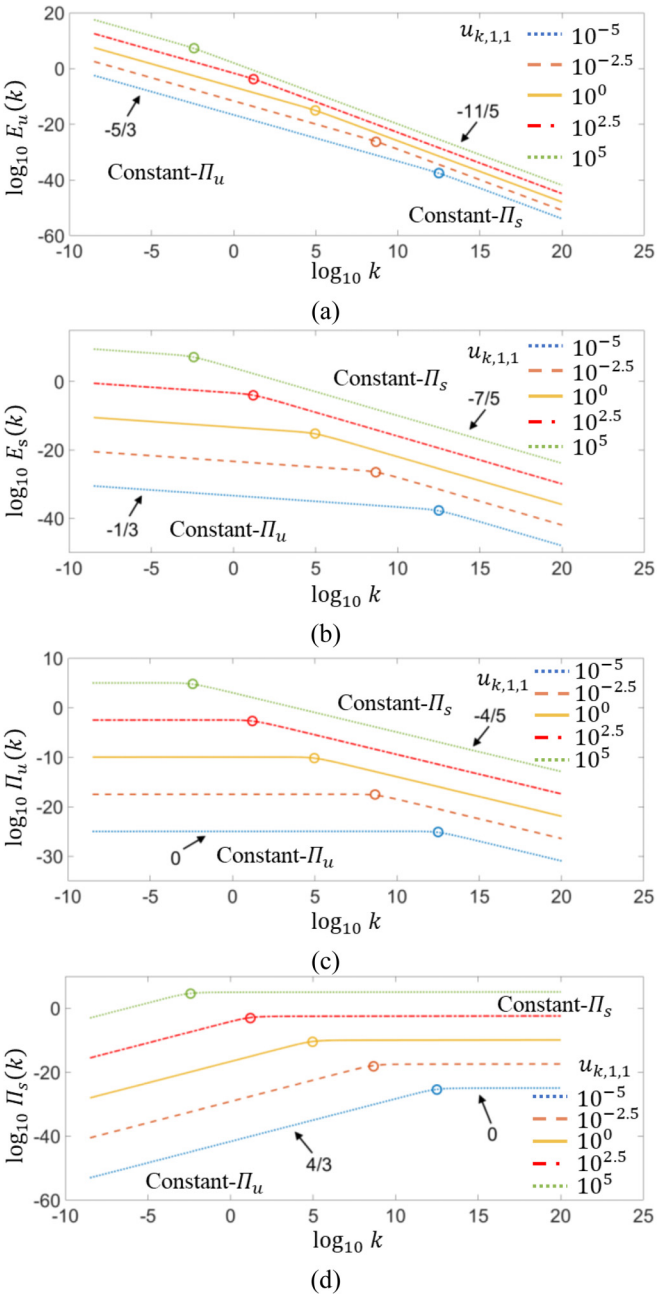

FIG. 4. Influence of $u_{k,1,1}$ on the transport of kinetic energy and scalar variance, where $\beta = 0$ and $MN = 1$. The colored circles denote the position of k_{ci}. (a) Power spectra of kinetic energy E_u. (b) Power spectra of scalar variance E_s. (c) Flux of kinetic energy Π_u. (d) Flux of scalar variance Π_s.

increased from 0 to 1, φ decreases rapidly from -1.5 (at $\beta = 0$) to -6 (at $\beta = 1$). As β is further increased to 5/4, ψ is decreased to -22.7.

After taking the influence of both MN and $u_{k,1,1}$ into account, it is obtained that $k_{ci} \sim (MN)^{\varphi} u_{k,1,1}^{\psi}$. The direct relationship between $u_{k,1,1}$ and MN (or the related dimensionless

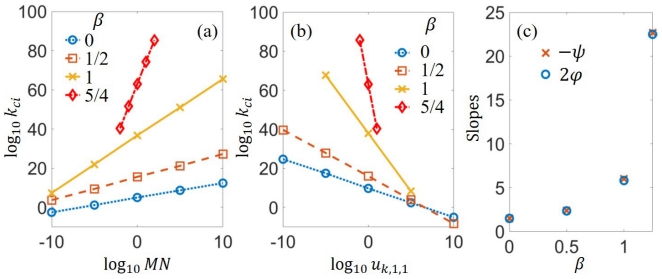

FIG. 5. Critical wave number k_{ci} varies with MN and $u_{k,1,1}$ for different β. (a) k_{ci} vs MN at $u_{k,1,1} = 1$. (b) k_{ci} vs $u_{k,1,1}$ at $MN = 1$. (c) Comparison between 2φ and $-\psi$.

parameters, e.g., Richardson number or Froude number in stratified turbulence [22–24]) relies on the physical problem and the dynamic system. It should be determined through either experiments or numerical simulations. For instance, if $u_{k,1,1} \sim (MN)^{1/3}$, considering $\psi \approx -2\varphi$ in this investigation, one simply has $k_{ci} = (MN)^{\varphi/3}$. In such a case, k_{ci} increases with MN and the constant-Π_u subrange moves toward a higher wave-number region, accompanied by a lifting of E_u. It means when the forced convection effect is stronger, larger kinetic energy and stronger velocity fluctuations are produced by forcing. Accordingly, it is more possible to induce a wider inertial subrange, through either direct or inverse cascade.

(iv) Zhao and Wang [11] showed that when $\beta > 2/3$, the kinetic energy in the constant-Π_s subrange in the high wave-number region is directly dissipated in the dissipation subrange. According to this investigation, the above conclusion is true in the range $2/3 < \beta < 3/2$ and $2 < \beta \leqslant 4$. There exists a new crossover wave number k_{us} which connects the constant-Π_s subrange and the dissipation subrange, where both the energy feeding rate and scalar feeding rate are balanced by the energy and scalar dissipation respectively. To get k_{us}, the following two conditions must be satisfied simultaneously:

$$\begin{aligned} F_s(k_{us}) &= D_u(k_{us}), \\ F_A(k_{us}) &= D_s(k_{us}). \end{aligned} \tag{26}$$

After simple processing, Eq. (26) becomes

$$\begin{aligned} M\left[E_s^{1/2}(k_{us})E_u^{-1/2}(k_{us})k_{us}^{\beta-2}\right] &= 2\nu, \\ N\left[E_s^{-1/2}(k_{us})E_u^{1/2}(k_{us})k_{us}^{-2}\right] &= 2D_f, \end{aligned} \tag{27}$$

which subsequently leads to

$$k_{us} = \left(\frac{MN}{4\nu D_f}\right)^{1/(4-\beta)} \tag{28}$$

For instance, in electrokinetic (EK) turbulence where $\beta = 1$, $M = \varepsilon E^2/\rho\langle\sigma\rangle$ and $N = \Delta\sigma/L$, $k_k = (\mathrm{Ra}_e/L^3)^{1/3}$, where $\mathrm{Ra}_e = \frac{\varepsilon E^2 L^2 \Delta\sigma}{4\nu D_f \rho\langle\sigma\rangle}$ is an electric Rayleigh number (see Baygents and Baldessari [25]) and L is a characteristic large scale. Interestingly, from Eq. (28), it can be seen that a singularity emerges at $\beta = 4$. When β is over 4, the exponent becomes negative and k_{us} increases with ν and D_f. This is unreasonable in a physical system under a certain equilibrium state, since a smaller ν should provide a larger k_{us}. In other words, if in a forced turbulent system with $\beta > 4$, the system could be unstable and crash, until a new equilibrium state with $\beta < 4$ is reestablished. Thus, in an equilibrium system, it is necessary to claim that $\beta \leqslant 4$, which is again coincident with Zhao and Wang [11]. When $\beta = 4$, k_{us} is infinite and unachievable.

In the investigation of Zhao and Wang [11], they also advanced a small length scale l_K. It should be noted that k_{us} is not the wave number corresponding to l_K. l_K, or the corresponding wave number k_K, can be obtained by merely $F_s(k_K) = D_u(k_K)$, while k_{us} is obtained from Eq. (26). In EK turbulence where $\beta = 1$, the former has $k_K \sim \mathrm{Ra}_e^{5/12}$ and the latter has $k_{us} \sim \mathrm{Ra}_e^{1/3}$.

C. Influence of the *i*th solution

Equation (19) is a third-order equation of $u_{k,i}$. It has three solutions in total, including one real solution and two complex solutions. In the investigation of Alam *et al.* [8], they solved the fifth-order equation [Eq. (30) in their paper] but only kept the real solution. However, as explained above, considering $E_u = k^{-1}(u_k u_k^*)$, the complex solutions of u_k can also lead to real E_u. Thus, it is necessary to revisit the roles of complex solutions of u_k in the turbulent transport. It should be noted that Eq. (30) in Alam *et al.* [8] has five solutions with only three of them being independent. The independent solutions in their investigation are exactly the same as our numerical calculation on Eq. (19) with $\beta = 0$.

From Fig. 6, it can be seen that the second and third solutions both exhibit a single slope in the MFD subrange. For the second solution, when $\beta < 3/2$, there is no constant flux of kinetic energy and scalar variance. As an example, at $\beta = 0$, $\xi_u = \xi_s = -3$ [Figs. 6(a) and 6(b)] and $\lambda_u = \lambda_s = -2$ [Figs. 6(c) and 6(d)]. However, when $\beta \geqslant 3/2$, the second solution exhibits a single constant-Π_u subrange, where $\xi_u = -5/3$ and $\lambda_u = 0$. ξ_s and λ_s can be calculated by Eqs. (21) and (22), while for the third solution, there is always a constant-Π_s subrange with $\lambda_s \approx 0$, where ξ_u, λ_u, and ξ_s can be calculated from Eqs. (23)–(25), for instance, when $\beta = 0$, $\xi_u = -11/5$, $\xi_s = -7/5$, and $\lambda_u = -4/5$ respectively.

The investigations on the additional solutions show some unpredicted results that may explain some early experimental observations. For instance, in stratified turbulence ($\beta = 0$) in the atmosphere, a -3 slope of the kinetic energy spectrum has been experimentally observed by Nastrom and Gage [26,27] on a synoptic scale. A later investigation by numerical simulation [28] shows that both the spectra of kinetic energy and potential energy (equivalent to density variance) have -3 slopes. The researchers focus on how the -3 spectra are generated (e.g., upscale or downscale cascade), but do not explain why there should be -3 spectra intrinsically. This investigation indicates the -3 spectra of kinetic energy and scalar variance are direct consequences of an inherent solution of the conservation equation [Eqs. (17) or (19)]. It must appear if some transitional conditions are satisfied.

IV. ASYMPTOTIC ANALYSIS

Part of the results from numerical calculation can also be achieved through asymptotical analysis, if rewrite Eq. (17) in the following manner:

$$\frac{du_k}{dk} = -\frac{u_k}{k}\frac{1+(3-2\beta)A(k)}{3+5\,A(k)}, \tag{29}$$

where $A(k) = k^{2-\beta}\frac{u_k^2}{MN}$. Let $u_k \sim k^{f(\beta)}$; with $f(\beta)$ being a scaling exponent relying on β, it is obtained that

$$f(\beta) = \frac{d\ln u_k}{d\ln k} = -\frac{1+(3-2\beta)A(k)}{3+5\,A(k)}. \tag{30}$$

On one hand, when $A(k)$ approaches 0, $f(\beta) = -1/3$, which in turn leads to $\xi_u = -5/3$ according to Eq. (15a). This is exactly what is found in the constant-Π_u subrange. On the other hand, when $A(k)$ approaches infinity, $f(\beta) = (2\beta-3)/5$, which in turn leads to $\xi_u = (4\beta-11)/5$. This is consistent with Eq. (22) in the constant-Π_s subrange.

When $\beta = 2$, $f(\beta) = 0$ as can be seen from the numerical simulation above. Accordingly, $A(k) = (MN)^{-1}$ and $f(2) = -\frac{1-(MN)^{-1}}{3+5\,(MN)^{-1}}$. It is interesting to see that, if $MN = 1$, $f(2)$ is exactly

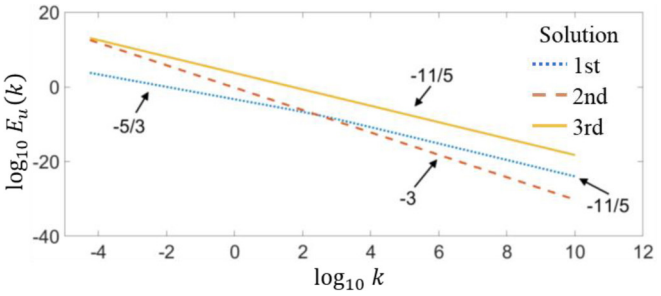

(a)

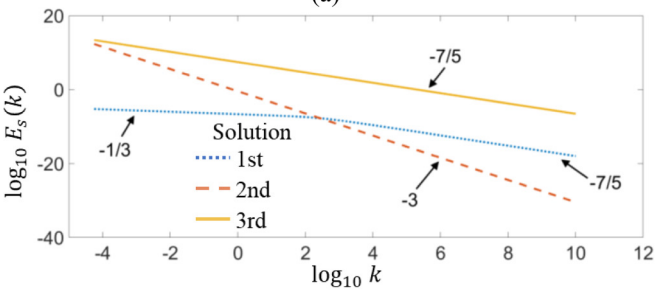

(b)

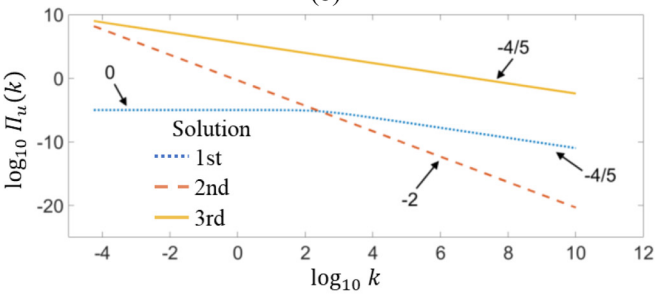

(c)

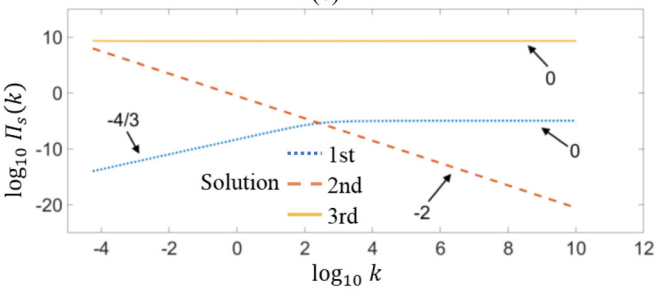

(d)

FIG. 6. Influence of the ith solution, where $M = N = 1$, $\beta = 0$. (a) Power spectra of kinetic energy E_u. (b) Power spectra of scalar variance E_s. (c) Flux of kinetic energy Π_u. (d) Flux of scalar variance Π_s.

zero. This explains why in the numerical simulation, there are special and singular scaling exponents at $\beta = 2$.

In fact, the special and singular case requires Eq. (30) to be established for all k. The case exists if two conditions are satisfied simultaneously. One is $f(\beta) = (\beta-2)/2$, the other is $MN = (\beta-4)/(4-3\beta)$. Since $MN > 0$, the special and singular case only exists in the range

TABLE II. Cascade processes in the scalar-based forced turbulence.

Features		
Π_u	Π_s	Related subranges
constant	constant	inertial subrange MFD subrange of the first solution when $\beta = 2/3$
quasiconstant	nonconstant	constant-Π_u subrange
nonconstant	quasiconstant	constant-Π_s subrange
nonconstant	nonconstant	dissipation subrange MFD subrange of the second solution when $\beta < 3/2$

of $4/3 < \beta < 4$. For each β in the range, a special MN can be found to reach the singular scaling exponents which are $\xi_u = \beta - 3$, $\xi_s = -3$, $\lambda_u = \frac{3}{2}\beta - 2$, and $\lambda_s = \frac{1}{2}\beta - 2$. It should be noted that in practical applications, it is almost impossible to reach the singular scaling exponents, since MN cannot be exactly $(\beta-4)/(4-3\beta)$. Accordingly, the subrange returns to constant-Π_s at the β.

V. DISCUSSION

To this end, four different cascade processes have been predicted theoretically in the scalar-based forced turbulence, with either constant or nonconstant fluxes of kinetic energy and scalar variance. The results are summarized in Table II.

The observation of the four cascade processes relies on the employment of the $\boldsymbol{M}\nabla^\beta s'$ type force. The quantity $\nabla^\beta s'$ qualitatively describes the relation between the multiscale force and the scalar fluctuation s'. The notation ∇^β is used to describe a βth order derivative, which can be $\frac{\partial^\beta}{\partial x^\beta}$, $\frac{\partial^\beta}{\partial y^\beta}$, $\frac{\partial^\beta}{\partial z^\beta}$, $\frac{\partial^\beta}{\partial x^{\beta_1}\partial y^{\beta_2}\partial z^{\beta_3}}$ (where $\beta = \beta_1 + \beta_2 + \beta_3$) or their combinations. For instance, when $\beta = 1$, the notation ∇^β can be $\frac{\partial}{\partial x}$, $\frac{\partial}{\partial y}$, etc. An example is in the EK turbulence model studied by Zhao and Wang [9,10], where $\frac{\partial}{\partial y}$ was applied. When $\beta = 2$, ∇^β can be $\frac{\partial^2}{\partial x^2}$, $\frac{\partial^2}{\partial x \partial y}$, etc. When $\beta = 3$, an example is the Cahn-Hilliard equation accompanied by hydrodynamic influence, where the ∇^β term has a format of $\nabla\nabla^2$ [see Eq. (240) of Verma [12]]. However, defining the property of β is difficult. From the spectral format of Eq. (5c), it is appropriate to define β as any real number no more than 4, including the fractional number and even negative number if physically appropriate. Defining the explicit form of ∇^β in real space is beyond the focus of this investigation. I hope to leave this question for the future.

The current model provides an effective tool to classify the turbulence driven by the scalar-based multiscale force, since the same or similar β in different turbulent systems reserve the same or similar transport process of kinetic energy and scalar variance. For instance, if we let $\beta = 1$, $\xi_s = -7/3$ in the constant-Π_u subrange which is exactly coincident with the density spectrum in magnetohydrodynamic (MHD) turbulence predicted by Batchelor in terms of pressure fluctuations [29–31]. Interestingly, if one slightly changes β to 0.9, it can be seen that $\xi_s = -2.13$ in the constant-Π_u subrange and $\xi_s = -1.76$ in the constant-Π_s subrange. These values are tightly close to the findings (-2.2 and -1.7) of Kowal *et al.* [32] on the density fluctuations in MHD turbulence. Therefore, $\beta \approx 1$ can characterize both EK (theoretical models by Zhao and Wang [9–11]) and MHD turbulence. When $\beta = 3$, the model could also be applicable (at least partially) for the Cahn-Hilliard equation accompanied by hydrodynamic influence [see Eq. (240) of Verma [12], if the binary mixtures have small scalar fluctuations and small gradients of the

mean scalar field. A $-5/3$ slope has been reported by Perlekar [33] in the kinetic energy spectra. However, it remains debated whether the $-5/3$ spectrum belongs to the inertial subrange, or the constant-Π_u subrange predicted in this model. One more example is when $\beta = -1$, $\xi_u = -3$ and $\xi_s = -1$ in the constant-Π_s subrange are approaching exponents in the elastic turbulence [34], which is intrinsically a chaotic flow [35]. If $\beta > 4$ indicates the crash of the statistical equilibrium state of the forced turbulence, $\beta \leqslant -1$ indicates that the forced turbulence degrades to chaotic. Thus, the model advanced in this investigation is restricted in the range $-1 < \beta \leqslant 4$, if in a stricter sense. The model provides us with a more general approach to distinguishing different scalar-based forced turbulence. Instead of seeking the solution to each type of turbulence, researchers can numerically solve the conceptual model in Eqs. (3a)–(3c) with β for general solutions.

VI. CONCLUSIONS

In this paper, the transport of kinetic energy and scalar variance in the turbulence driven by scalar-based multiscale force has been theoretically investigated. In this type of turbulence, the scalar field is strongly coupled with the velocity field and dominated by active transport. A conservative equation relying on the fluxes of kinetic energy and scalar variance has been established. The equation has three solutions, including one real solution and two complex solutions. Based on the solutions, a comprehensive cascade picture has been established for this type of turbulence.

The investigations on the real solution indicate that the turbulence has four types of cascade processes, depending on whether the fluxes of kinetic energy and scalar variance are constant or not. In the inertial subrange, both the fluxes of kinetic energy and scalar variance are constant. In the constant-Π_u or constant-Π_s subranges, only the flux of kinetic energy or scalar variance is quasiconstant. And in the dissipation subrange, both the fluxes of kinetic energy and scalar variance are nonconstant.

The scaling exponents in the power spectra of kinetic energy and scalar variance strictly depend on the order of derivatives, i.e., β. In the constant-Π_u subrange, ξ_u is always $-5/3$, while $\xi_s = -(6\beta + 1)/3$. In the constant-Π_s subrange, $\xi_u = (4\beta - 11)/5$ and $\xi_s = -(2\beta + 7)/5$ which are both consistent with the theory of Zhao and Wang [11]. Relying on β, the transport of kinetic energy and scalar variance can be distinguished as four cases. (1) When $\beta < 3/2$ (except $\beta = 2/3$), the constant-Π_u and constant-Π_s subranges both exist in the investigated wave-number region, and the former locates on the lower wave-number side of the latter. If $\beta = 2/3$, the constant-Π_u and constant-Π_s subrange overlap and form a new inertial subrange, where both ξ_u and ξ_s equal $-5/3$. (2) When $3/2 \leqslant \beta < 2$, only the constant-Π_u subrange is observed. (3) At $\beta = 2$, if $MN = 1$, special and singular exponents of $\xi_u = -1$, $\xi_s = -3$, $\lambda_u = 1$, and $\lambda_s = -1$ can be found. Otherwise, if $MN \neq 1$, the constant-Π_s subrange is observed. (4) When $2 < \beta \leqslant 4$, only the constant-Π_s subrange is observed. Note that $\beta = 4$ is a critical point for the equilibrium state to be established. Beyond this, the equilibrium state of the turbulence system could be crashed.

The influence of MN and the initial value of the real solution $u_{k,1,1}$ on the crossover wave number between the constant-Π_u and constant-Π_s subranges are also investigated in the range $\beta < 3/2$ (except $\beta = 2/3$). The results indicate $k_{ci} \sim (MN)^{\varphi} u_{k,1,1}^{\psi}$, with $\varphi > 0$ and $\psi < 0$. It is interesting that $\psi \approx -2\varphi$. The larger the β is, the larger $|\psi|$ and φ. Another microscale $k_{us} = (MN/4\nu D_s)^{1/(4-\beta)}$ is also predicted if the constant-Π_s subrange is present. On k_{us}, the energy feeding rate and scalar feeding rate are simultaneously balanced by the energy and scalar dissipation respectively. The formula of k_{us} prevents β to be larger than 4.

The results above are all for the first solution. For the second solution, when $\beta < 3/2$, there is no constant flux of kinetic energy and scalar variance. When $\beta \geqslant 3/2$, a single constant-Π_u subrange is predicted, while for the third solution, there is always a constant-Π_s subrange with $\lambda_s \approx 0$.

This paper aims to establish a comprehensive picture of the cascade process in the forced turbulence driven by scalar-based multiscale force and the accompanied active transport process, within a unified theoretical frame. In the meanwhile, I hope this investigation can significantly deepen our understanding of the transport of kinetic energy and scalar variance, e.g., in stratified turbulence, electrokinetic turbulence, and other physical systems like condensed matter physics. The scalar is not restricted to any known physical quantities, e.g., temperature, density, electric conductivity, and permittivity, etc., but also includes broad scalar quantities like information.

ACKNOWLEDGMENT

The investigation was supported by National Nature Science Foundation of China Grant No. 11672229. I appreciate the suggestions of the reviewers on improving the manuscript.

[1] R. Bolgiano, Turbulent spectra in a stably stratified atmosphere, J. Geophys. Res. **64**, 2226 (1959).
[2] A. M. Obukhov, On the influence of Archimedean forces on the structure of the temperature field in a turbulent flow, Dokl. Akad. Nauk. SSR **125**, 1246 (1959).
[3] J. J. Niemela, L. Skrbek, K. R. Sreenivasan, and R. J. Donnelly, Turbulent convection at very high rayleigh numbers, Nature (London) **404**, 837 (2000).
[4] D. Lohse and K.-Q. Xia, Small-Scale properties of turbulent rayleigh-bénard convection, Annu. Rev. Fluid Mech. **42**, 335 (2010).
[5] A. Kumar, A. G. Chatterjee, and M. K. Verma, Energy spectrum of buoyancy-driven turbulence, Phys. Rev. E **90**, 023016 (2014).
[6] R. Benzi, L. Biferale, S. Ciliberto, M. V. Struglia, and R. Tripiccione, Generalized scaling in fully developed turbulence, Physica D (Amsterdam, Neth.) **96**, 162 (1996).
[7] P. A. Davidson, *Turbulence in Rotating, Stratified and Electrically Conducting Fluids* (Cambridge University Press, New York, 2013).
[8] S. Alam, A. Guha, and M. K. Verma, Revisiting bolgiano–obukhov scaling for moderately stably stratified turbulence, J. Fluid Mech. **875**, 961 (2019).
[9] W. Zhao and G. Wang, Scaling of velocity and scalar structure functions in ac electrokinetic turbulence, Phys. Rev. E **95**, 023111 (2017).
[10] W. Zhao and G. Wang, Cascade of turbulent energy and scalar variance in DC electrokinetic turbulence, Physica D (Amsterdam, Neth.) **399**, 42 (2019).
[11] W. Zhao and G. Wang, A tentative study of the transport of energy and other scalar quantities in forced turbulence driven by $\nabla^n A$ − type volume forces, J. Hydrodyn. Ser. B (Eng. Ed.) **33**, 1271 (2021).
[12] M. K. Verma, Variable energy flux in turbulence, J. Phys. A: Math. Theor. **55**, 013002 (2022).
[13] G. Wang, F. Yang, and W. Zhao, There can be turbulence in microfluidics at low reynolds number, Lab Chip **14**, 1452 (2014).
[14] G. Wang, F. Yang, and W. Zhao, Microelectrokinetic turbulence in microfluidics at low reynolds number, Phys. Rev. E **93**, 013106 (2016).
[15] D. Nath, A. Pandey, A. Kumar, and M. K. Verma, Near isotropic behavior of turbulent thermal convection, Phys. Rev. Fluids **1**, 064302 (2016).
[16] M. K. Verma, Statistical theory of magnetohydrodynamic turbulence: recent results, Phys. Rep. **401**, 229 (2004).
[17] M. K. Verma, *Physics of Buoyant Flows: From Instabilities to Turbulence* (Hackensack, New Jersey, 2018).
[18] A. N. Kolmogorov, The local structure of turbulence in incompressible viscous fluid for very large reynolds numbers, Dokl. Akad. Nauk SSSR **30**, 301 (1941) [Proc. R. Soc. Lond. A **434**, 9 (1991)].
[19] U. Frisch, *Turbulence—The Legacy of A. N. Kolmogorov* (Cambridge University Press, New York, 1995).

[20] A. M. Obukhov, Structure of the temperature field in a turbulent flow, Izv. Akad. Nauk. SSSR Ser. Geog. Geofiz. **13**, 58 (1949).
[21] S. Corrsin, On the spectrum of isotropic temperature fluctuations in an isotropic turbulence, J. Appl. Phys. **22**, 469 (1951).
[22] C. J. Howland, J. R. Taylor, and C. P. Caulfield, Mixing in forced stratified turbulence and its dependence on large-scale forcing, J. Fluid Mech. **898**, A7 (2020).
[23] A. Maffioli and P. A. Davidson, Dynamics of stratified turbulence decaying from a high buoyancy reynolds number, J. Fluid Mech. **786**, 210 (2016).
[24] S. Okino and H. Hanazaki, Direct numerical simulation of turbulence in a salt-stratified fluid, J. Fluid Mech. **891**, A19 (2020).
[25] J. C. Baygents and F. Baldessari, Electrohydrodynamic instability in a thin fluid layer with an electrical conductivity gradient, Phys. Fluids **10**, 301 (1998).
[26] G. D. Nastrom, K. S. Gage, and W. H. Jasperson, The atmospheric kinetic energy spectrum, 10^0–10^4 km, Nature (London) **310**, 36 (1984).
[27] G. D. Nastrom and K. S. Gage, A climatology of atmospheric wavenumber spectra of wind and temperature observed by commercial aircraft, J. Atmospheric Sci. **42**, 950 (1985).
[28] Y. Kitamura and Y. Matsuda, The $k_H{}^{-3}$ and $k_H{}^{-5/3}$ energy spectra in stratified turbulence, Geophys. Res. Lett. **33**, L0580 (2006).
[29] G. K. Batchelor, Pressure fluctuations in isotropic turbulence, Math. Proc. Cambridge Philos. Soc. **47**, 359 (1951).
[30] D. Montgomery, M. R. Brown, and W. H. Matthaeus, Density fluctuation spectra in magnetohydrodynamic turbulence, J. Geophys. Res. **92**, 282 (1987).
[31] D. Biskamp, *Magnetohydrodynamic Turbulence* (Cambridge University Press, Cambridge, UK, 2003).
[32] G. Kowal, A. Lazarian, and A. Beresnyak, Density fluctuations in MHD Turbulence: Spectra, Intermittency, and topology, Astrophys. J. **658**, 423 (2007).
[33] P. Perlekar, Kinetic energy spectra and flux in turbulent phase-separating symmetric binary-fluid mixtures, J. Fluid Mech. **873**, 459 (2019).
[34] A. Groisman and V. Steinberg, Elastic turbulence in a polymer solution flow, Nature (London) **405**, 53 (2000).
[35] V. Steinberg, Scaling Relations in Elastic Turbulence, Phys. Rev. Lett. **123**, 234501 (2019).